An approach to assess the thermal aging effects on the coupling between inelasticity and network alteration in filled rubbers

M. Chaabane, N. Ding, Fahmi Zairi

Version of Record: https://www.sciencedirect.com/science/article/pii/S0020746221001177
Manuscript_24ffd3f99a08ec1306d9ba2cde3052e7

An approach to assess the thermal aging effects on the coupling between inelasticity and network alteration in filled rubbers

Makram Chaabane[a], Ning Ding[b], Fahmi Zaïri[c*]

[a]Monastir University, ENIM, Mechanical Engineering Laboratory, 5019 Monastir, Tunisia
[b]Qilu University of Technology (Shandong Academy of Sciences), Engineering Research Center of Failure Analysis and Safety Assessment, Shandong Analysis and Test Center, 250014 Jinan, China
[c]Lille University, Civil Engineering and geo-Environmental Laboratory (ULR 4515 LGCgE), 59000 Lille, France

*Corresponding author.
E-mail address: fahmi.zairi@polytech-lille.fr

Abstract

The development of a constitutive representation for predicting the durability of filled rubbers upon aggressive environmental conditions is crucial for numerous technical examples but still remains largely an open issue. This paper presents a constitutive model for the prediction of thermal aging effects on the inelastic response of filled rubbers. A network alteration theory is proposed for the thermally driven network degradation by considering a collection of chemical and physical changes occurring inside the rubber-filler material system. The network decomposition considers scission-rebound mechanisms of links (between filler aggregates and between elastically active cross-linked chains) and changes in movements of the free chains superimposed into the (newly born and original) chemically linked network. The material kinetics is designed using multi-step (physical) stress relaxation experiments performed at room temperature on a sulfur-vulcanized styrene-butadiene rubber containing different amounts of carbon-black fillers, and previously submitted to an accelerated chemical stress relaxation procedure, i.e. aging at constant stretch for various temperatures and exposure times. The time-temperature equivalence principle is used to construct master curves of the alteration kinetics for both the cross-linked chains and the superimposed free chains. The amplified effect of the fillers is also considered in our network decomposition to account for the cross-linked chains/fillers interactions and the free chains/fillers interactions. The capabilities of the proposed network alteration based constitutive model to describe and predict the material response evolution in terms of stiffening, hysteresis area increase and physical relaxation increase are shown. The chemically induced "plastic-like" deformation and stress relaxation are predicted using the developed model. The results show the importance of the inelastic effects on the prediction of long-term material response due to thermally activated degradation. From an applicative point of view, the model makes possible to estimate the operational life of pre-strained rubber mechanical components with respect to loss of pressure and flexibility.

Keywords: Elastomeric materials; Thermal aging; Chemical relaxation; Physical relaxation; Filler effects.

1. Introduction

Rubbers used in engineering applications are submitted to relatively mild aging conditions or aggressive environmental conditions such as light, humidity, gamma irradiation and elevated temperature. Establishing the connection between the aging-induced degradation of the rubber network and the material response evolution with aging remains the major obstacle in any non-empirical approach for predicting the durability of rubber mechanical components. This contribution is focused on thermally aged rubbers. This type of aging is termed chemical aging in the sense that it affects the chemical structure of the material in an unrecoverable manner.

The description of the rubber response evolution with thermal aging in a physically consistent way requires the development of constitutive models with a detailed understanding of the aging-induced structural alterations that govern the mechanical response. The chemical aging leads to a collection of competing events occurring in the cross-linked network, namely, scission of links and cross-linking formations, that depend on a multitude of factors such as rubber formulation (antioxidants, fillers, etc.), temperature and exposure time [1-4]. In filled rubbers, in which the agglomeration of fillers plays an important role in the material response, the thermal aging increases the number of inter-aggregates links as evidenced by electrical conductivity studies [5]. As a basic understanding of the molecular alteration due to scission and cross-linking events, the changes of the average chain length and chain density alter the elastic properties [6] and the ultimate properties [7] of the rubber. By contrast, the influence of the thermal aging degradation on the inelastic response of rubber is imprecisely understood to date. It is well recognized that the inelastic features in the rubber gum are due to the recoverable viscoelastic motion of free (FR) chains that are superimposed on a network of elastically active cross-linked (CL) chains. When fillers are introduced in the rubber matrix, the viscous sliding between fillers and filler-rubber matrix and the breakdown-rebound

mechanism of inter-aggregates links play a significant role in the inelastic effects. These recoverable viscoelastic mechanisms are responsible for (physical) stress relaxation during a constant stretch and for stress hysteresis (distinct loading and unloading paths) during a cyclic loading. Especially for many technical applications such as seals and connectors, rubber has to maintain a constant pressure at high temperature and the aging-induced changes in the relaxation response must be considered to evaluate the operational life of the mechanical component. In this case, the concept of a dual molecular network was invoked by Tobolsky and coworkers [8] to explain the decay towards zero of the stress during relaxation of rubber at high temperature. The latter relaxation was termed chemical relaxation due to unrecoverable molecular changes manifested by the presence of a "plastic-like" (permanent deformation) deformation upon complete unloading [9]. The continuous decrease in stress being proportional to the changes of the average chain density, the rubber is conceptually regarded as two superimposed networks with relative densities that change over time: an original CL network (at equilibrium when rubber is un-stretched) and a newly born CL network (at equilibrium when rubber is stretched) created by the breakdown-rebound mechanism of links in a stress free state. The concept of a double network was proved by experiments [10-12] or molecular dynamics simulations [13-14]. The concept provides a relevant molecular description of the elastically active CL chains leading to the chemical stress relaxation effects. Nonetheless, the continuous stress decrease includes also physical stress relaxation effects due to recoverable viscoelastic motion of FR chains but their aging-induced alteration is not defined to date. In other applications, rubber is exposed to cyclic loading at high temperature due to thermal environmental and/or to self-heating which manifests by an increase in temperature inside the material. The modifications in the fatigue response due to thermal aging effects reported in the literature [15] may be attributed to the alteration of elastically active CL chains, responsible for the purely elastic and ultimate

properties, but also to the alteration of FR chains responsible for the inelastic effects and especially the hysteretic response. The aging-induced changes in the mechanical energy, converted in a large part into dissipative self-heating [16-17], could significantly impact the fatigue life of rubber [18]. Nonetheless, the way aging affects the inelastic effects is not established to date.

The constitutive representation of the intrinsic behavior of rubbers in response to a mechanical loading is a constant concern and an active research area. Despite the effective role of the aging degradation on the mechanical response and the large number of examples of mechanical components submitted to aggressive environmental conditions, a literature survey shows that there exist very few contributions dealing with the constitutive modeling of aged polymers [2, 19-29]. Although an intensification of publications in the literature can be found over the last decade, the current theoretical works introduce the chemically induced unrecoverable mechanisms but generally ignore the inelastic effects. To date, there is no constitutive representation of the impact of aging-induced degradation on the recoverable inelastic movements. In order to describe the material response evolution in a physically consistent way, the constitutive model has to represent the aging effects on the material response in combination with the inelastic effects and the aging-induced structural modifications.

In the present contribution, we intend to propose a constitutive model to describe the time-dependent material behavior of thermally aged rubbers. The outline of the present paper is as follows. In Section 2, we present the constitutive equations in the framework of nonlinear continuum mechanics combined with the proposed network alteration theory. In Section 3, we present the experimental evidences which characterize the thermal aging effects on the time-dependent material response of the selected rubber containing different filler fractions. The material kinetics is designed and used to highlight the filler effects on the degradation

mechanisms of the thermally aged rubber-filler material system. The predictive capabilities of the model are also shown. Finally, some concluding remarks are formulated in Section 4.

The following notation is used throughout the text. Tensors and vectors are denoted by normal boldfaced letters and italicized boldfaced letters, respectively, while scalars and individual components of vectors and tensors are denoted by normal italicized letters. The superposed dot designates the loading time derivative and the superscript *T* designates the transpose.

2. Model formulation

The rubber gum is modeled as a two-network medium constituted by randomly oriented and distributed elastically active chains, interlinked with reticulation nodes (cross-links), on which FR chains are superimposed. At the macroscopic scale, the entropic resistance to deformation of the elastically active CL chains leads to the nonlinear purely elastic response of the rubber gum. The FR chains, superimposed across the CL network, provide to the rubber gum the viscous features and capture the physical relaxation mechanisms[1]. A constitutive model is derived based upon this network decomposition to describe the time-dependent material response of thermally aged rubbers in the framework of nonlinear continuum mechanics. The material response changes due to thermal aging are related to the alteration of the network structure by considering the kinetics of the degradation mechanisms. In the present alteration theory, the evolution in elastically active CL chains and the resulting changes in movements of the superimposed FR chains are considered to reflect the degradation state of the rubber network.

[1] The FR chains contribute to additional resistance to deformation but have lower resistance than the CL chains. They have the capability to significantly modify their conformation. If the material is stretched at a high enough rate, both CL chains and FR chains motion affinely. When the material is held in the stretched state, the CL network is the stretched configuration but the FR chains tend to slowly return to a more relaxed configuration.

2.1. General structure

In this section, the general structure of the constitutive model is detailed. In line with our network decomposition, the CL and FR chains act in parallel in the model as rheologically schematized in Fig. 1. Before to present the constitutive relationships, the thermodynamical foundations restricting the proposed model are stated. Let us start to define the usual deformation gradient $\mathbf{F}=\partial \boldsymbol{x}/\partial \boldsymbol{X}$ mapping material points labeled with $\mathbf{X}$ in the reference configuration Ω_0 to their actual position $\mathbf{x}$ in the deformed configuration Ω with the Jacobian $J=\det\mathbf{F}>0$. The time derivative of the deformation gradient is $\dot{\mathbf{F}}=\mathbf{L}\mathbf{F}$ where $\mathbf{L}$ is the gradient of the spatial velocity. The parallel scheme of the model imposes that the deformation of the CL chains $\mathbf{F}_{\mathrm{CL}}$ is identical to that of the FR chains $\mathbf{F}_{\mathrm{FR}}$: $\mathbf{F}_{\mathrm{CL}}=\mathbf{F}_{\mathrm{FR}}$. The second law of thermodynamics restricts the proposed model via the so-called Clausius-Duhem inequality. For an isothermal process, it can be expressed in the following reduced form of the dissipation function $\mathcal{D}$:

$$\mathcal{D}=\mathcal{P}-\dot{\psi}\geq 0,\ \mathcal{P}=\mathbf{S}:\frac{1}{2}\dot{\mathbf{C}}=\boldsymbol{\sigma}:\mathbf{D} \tag{1}$$

where Ψ is the Helmholtz free energy function per unit reference volume and $\mathcal{P}$ is the stress power expressed in terms of the second Kirchhoff stress $\mathbf{S}$ and the time derivative of the right Cauchy-Green $\mathbf{C}=\mathbf{F}^T\mathbf{F}$ in the Lagrangian description, or in terms of the symmetric Eulerian rate of the deformation $\mathbf{D}=\left(\mathbf{L}+\mathbf{L}^T\right)/2$ (with $\mathbf{L}=\dot{\mathbf{F}}\mathbf{F}^{-1}$) and the Cauchy stress $\boldsymbol{\sigma}$ in the Eulerian description. Only isochoric deformation processes are assumed. This material incompressibility assumption is implied by the fact that the bulk modulus of rubbers is generally fairly large in comparison with the shear modulus. Moreover, the inelastic volumetric response due to deformation-induced cavitation [30-31] is disregarded. The Jacobian J does not thus appear in the dissipation inequality (1) since it is equal to one. Non-dependence of the parameters vis-à-vis the aging temperature is also supposed. The presented

theory is based on an additive split of the Helmholtz free energy function ψ into two contributions:

$$\psi = \psi_{\mathrm{CL}} + \psi_{\mathrm{FR}} \tag{2}$$

where ψ_{CL} and ψ_{FR} denote the free energies for CL and FR networks, respectively, resulting from the contribution of the nonlinear elastic spring of the CL network and the Maxwell branch (nonlinear elastic spring in series with viscous damper) of the FR network. In the thermodynamic equilibrium state, the nonlinear elastic spring of the Maxwell branch is relaxed and the total free energy consists only to that of the CL network, i.e. $\psi = \psi_{\mathrm{CL}}$.

In the same manner, the Cauchy stress $\boldsymbol{\sigma}$ in the rubber gum is additively split:

$$\boldsymbol{\sigma} = \boldsymbol{\sigma}_{\mathrm{CL}} + \boldsymbol{\sigma}_{\mathrm{FR}} \tag{3}$$

where $\boldsymbol{\sigma}_{\mathrm{CL}}$ and $\boldsymbol{\sigma}_{\mathrm{FR}}$ are the respective Cauchy stresses.

Using Eqs. (2) and (3), the Clausius-Duhem inequality (1) becomes:

$$\mathcal{D} = \left(\boldsymbol{\sigma}_{\mathrm{CL}} + \boldsymbol{\sigma}_{\mathrm{FR}}\right) : \mathbf{D} - \left(\dot{\psi}_{\mathrm{CL}} + \dot{\psi}_{\mathrm{FR}}\right) \geq 0 \tag{4}$$

The two networks are a priori assumed to be independent and a stronger constraint can be then imposed to the proposed model by assuming that each should satisfy the dissipation inequality separately. Therefore, we can write the dissipation inequality in the following form:

$$\begin{aligned} \mathcal{D}_{\mathrm{CL}} &= \boldsymbol{\sigma}_{\mathrm{CL}} : \mathbf{D}_{\mathrm{CL}} - \dot{\psi}_{\mathrm{CL}} \geq 0 \\ \mathcal{D}_{\mathrm{FR}} &= \boldsymbol{\sigma}_{\mathrm{FR}} : \mathbf{D}_{\mathrm{FR}} - \dot{\psi}_{\mathrm{FR}} \geq 0 \end{aligned} \tag{5}$$

where the dissipation function $\mathcal{D}$ is additively split into two parts: $\mathcal{D} = \mathcal{D}_{\mathrm{CL}} + \mathcal{D}_{\mathrm{FR}} \geq 0$.

These general relations form a basis for the development of a suitable theory and are completed by a set of constitutive equations in the two next subsections.

2.1.1. Constitutive representation of the cross-linked (CL) chains

The Cauchy stress $\boldsymbol{\sigma}_{\mathrm{CL}}$ in the continuous network of CL chains is constitutively given by the Arruda-Boyce [32] relation based upon the eight-chain network of non-Gaussian chains:

$$\boldsymbol{\sigma}_{\mathrm{CL}} = \frac{n_{\mathrm{CL}} k_{\mathrm{B}} T}{3} \frac{\sqrt{N_{\mathrm{CL}}}}{\lambda_{\mathrm{CL}}} \mathrm{L}^{-1}\left(\frac{\lambda_{\mathrm{CL}}}{\sqrt{N_{\mathrm{CL}}}}\right)\left(\mathbf{B}_{\mathrm{CL}} - \lambda_{\mathrm{CL}}^2 \mathbf{I}\right) \tag{6}$$

where $\mathbf{I}$ is the identity tensor and λ_{CL} represents the average stretch on each chain of the CL network: $\lambda_{\mathrm{CL}} = \sqrt{\mathrm{trace}\left(\mathbf{B}_{\mathrm{CL}}\right)/3}$ in which $\mathbf{B}_{\mathrm{CL}} = \mathbf{F}_{\mathrm{CL}} \mathbf{F}_{\mathrm{CL}}^{T}$ is the left Cauchy-Green strain tensor. The term L^{-1} is the inverse Langevin function used to account for the limiting chain extensibility and the progressive stress increase at high stretch levels due to the entropic resistance to molecular network alignment. It can be approximated by the Padé approximation:

$$\mathrm{L}^{-1}\left(\frac{\lambda_{\mathrm{CL}}}{\sqrt{N_{\mathrm{CL}}}}\right) \approx \frac{\lambda_{\mathrm{CL}}}{\sqrt{N_{\mathrm{CL}}}} \frac{3N_{\mathrm{CL}} - \lambda_{\mathrm{CL}}^2}{N_{\mathrm{CL}} - \lambda_{\mathrm{CL}}^2} \tag{7}$$

Two fundamental physical-related quantities are introduced in the expression (6): the average number of CL chains per unit reference volume n_{CL} (i.e. average CL chain density) and the average number of connected rigid-links in a CL chain N_{CL} (i.e. average CL chain length). The product $C_{\mathrm{CL}} = n_{\mathrm{CL}} k_{\mathrm{B}} T$ defines the shear modulus at low stretch levels in which k_{B} is the Boltzmann's constant and T is the absolute temperature. When the limiting chain extensibility parameter approaches infinity in the relation (6), it reduces to the Neo-Hookean relation.

2.1.2. Constitutive representation of the free (FR) chains

The Cauchy stress $\boldsymbol{\sigma}_{\mathrm{FR}}$ in the discontinuous network of FR chains needs to be founded on the finite-strain viscoelasticity theory. The dual stress and strain tensors are constitutively

coordinated by a Neo-Hookean formulation in which the elastic left Cauchy-Green strain tensor $\mathbf{B}^{\mathrm{e}}_{\mathrm{FR}} = \mathbf{F}^{\mathrm{e}}_{\mathrm{FR}}\mathbf{F}^{\mathrm{e}^T}_{\mathrm{FR}}$ is the driving force:

$$\boldsymbol{\sigma}_{\mathrm{FR}} = 2C_{\mathrm{FR}}\left(\mathbf{B}^{\mathrm{e}}_{\mathrm{FR}} - \left(\lambda^{\mathrm{e}}_{\mathrm{FR}}\right)^2\mathbf{I}\right) \tag{8}$$

where $C_{\mathrm{FR}} = n_{\mathrm{FR}}k_{\mathrm{B}}T/2$ is the viscous parameter (n_{FR} being the average number of FR chains per unit volume), $\lambda^{\mathrm{e}}_{\mathrm{FR}} = \sqrt{\mathrm{trace}\left(\mathbf{B}^{\mathrm{e}}_{\mathrm{FR}}\right)/3}$ and $\mathbf{F}^{\mathrm{e}}_{\mathrm{FR}}$ is the elastic deformation gradient whose the history dependence is expressed by using the basic concept of the deformation gradient separation introducing the notion of the intermediate (relaxed) configuration Ω_{relax} assumed stress-free as illustrated in Fig. 2a. The deformation gradient $\mathbf{F}_{\mathrm{FR}} = \mathbf{F}^{\mathrm{e}}_{\mathrm{FR}}\mathbf{F}^{\mathrm{v}}_{\mathrm{FR}}$ is multiplicatively decomposed into an elastic part $\mathbf{F}^{\mathrm{e}}_{\mathrm{FR}}$ and a viscous part $\mathbf{F}^{\mathrm{v}}_{\mathrm{FR}}$. The elastic and viscous parts, $\mathbf{L}^{\mathrm{e}}_{\mathrm{FR}}$ and $\mathbf{L}^{\mathrm{v}}_{\mathrm{FR}}$, of the corresponding kinematic rates additively split the velocity gradient $\mathbf{L}_{\mathrm{FR}} = \dot{\mathbf{F}}_{\mathrm{FR}}\mathbf{F}^{-1}_{\mathrm{FR}}$:

$$\mathbf{L}_{\mathrm{FR}} = \underbrace{\dot{\mathbf{F}}^{\mathrm{e}}_{\mathrm{FR}}\mathbf{F}^{\mathrm{e}^{-1}}_{\mathrm{FR}}}_{\mathbf{L}^{\mathrm{e}}_{\mathrm{FR}}} + \underbrace{\mathbf{F}^{\mathrm{e}}_{\mathrm{FR}}\dot{\mathbf{F}}^{\mathrm{v}}_{\mathrm{FR}}\mathbf{F}^{\mathrm{v}^{-1}}_{\mathrm{FR}}\mathbf{F}^{\mathrm{e}^{-1}}_{\mathrm{FR}}}_{\mathbf{L}^{\mathrm{v}}_{\mathrm{FR}}} \text{ and } \mathbf{L}^{\mathrm{v}}_{\mathrm{FR}} = \underbrace{\frac{1}{2}\left(\mathbf{L}^{\mathrm{v}}_{\mathrm{FR}} + \mathbf{L}^{\mathrm{v}^T}_{\mathrm{FR}}\right)}_{\mathbf{D}^{\mathrm{v}}_{\mathrm{FR}}} + \underbrace{\frac{1}{2}\left(\mathbf{L}^{\mathrm{v}}_{\mathrm{FR}} - \mathbf{L}^{\mathrm{v}^T}_{\mathrm{FR}}\right)}_{\mathbf{W}^{\mathrm{v}}_{\mathrm{FR}}} \tag{9}$$

in which the viscous velocity gradient $\mathbf{L}^{\mathrm{v}}_{\mathrm{FR}}$ characterizing constitutively the FR chains-induced inelastic effects is further additively decomposed into a viscous stretching rate $\mathbf{D}^{\mathrm{v}}_{\mathrm{FR}}$ and a viscous stretching rate $\mathbf{W}^{\mathrm{v}}_{\mathrm{FR}}$ which drops out, i.e. $\mathbf{W}^{\mathrm{v}}_{\mathrm{FR}} = \mathbf{0}$, if irrotationality of the viscous flow is assumed[2]. Thus, the viscous deformation gradient $\mathbf{F}^{\mathrm{v}}_{\mathrm{FR}}$ is extracted from: $\dot{\mathbf{F}}^{\mathrm{v}}_{\mathrm{FR}} = \mathbf{F}^{\mathrm{e}^{-1}}_{\mathrm{FR}}\mathbf{D}^{\mathrm{v}}_{\mathrm{FR}}\mathbf{F}^{\mathrm{e}}_{\mathrm{FR}}\mathbf{F}^{\mathrm{v}}_{\mathrm{FR}}$ in which the viscous stretching rate $\mathbf{D}^{\mathrm{v}}_{\mathrm{FR}}$ has the following general form:

$$\mathbf{D}^{\mathrm{v}}_{\mathrm{FR}} = \dot{\gamma}_{\mathrm{FR}}\frac{\boldsymbol{\sigma}'_{\mathrm{FR}}}{\sqrt{2}\left\|\boldsymbol{\sigma}_{\mathrm{FR}}\right\|},\ \left\|\boldsymbol{\sigma}_{\mathrm{FR}}\right\| = \sqrt{\frac{1}{2}\mathrm{trace}\left(\boldsymbol{\sigma}'_{\mathrm{FR}}\boldsymbol{\sigma}'_{\mathrm{FR}}\right)} \tag{10}$$

[2] The multiplicative decomposition of the deformation gradient implies that the unloading process (relating the deformed configuration with the relaxed configuration) is not uniquely defined. Indeed, an arbitrary rigid body rotation of the relaxed configuration still leaves the relaxed configuration stress free. One way to make unique the unloaded configuration, with no loss in generality, is to assume the inelastic flow irrotational.

where $\|\boldsymbol{\sigma}_{\mathrm{FR}}\|$ is the effective viscous shear stress and $\boldsymbol{\sigma}'_{\mathrm{FR}}$ is the deviatoric part of the Cauchy stress $\boldsymbol{\sigma}_{\mathrm{FR}}$.

The formalism used to describe the intrinsic response of FR chains is a viscoplasticity with no threshold allowing viscous components to develop as soon as the stress becomes non-zero [33] and to retain a remanent strain after mechanical unlading. The nonlinear stress-dependency of the effective viscosity can be described by an exponential law or a power law depending on an effective stress quantity [34]. The accumulated viscous strain rate $\dot{\gamma}_{\mathrm{FR}}$ is related to the motion of the FR chains and, as a matter of fact, depends nonlinearly on the level of viscous stress τ_{FR} and viscous stretch $\lambda^{\mathrm{v}}_{\mathrm{FR}}$:

$$\dot{\gamma}_{\mathrm{FR}} = \hat{\dot{\gamma}}_{\mathrm{FR}}\left(\|\boldsymbol{\sigma}_{\mathrm{FR}}\|, \lambda^{\mathrm{v}}_{\mathrm{FR}}\right),\ \lambda^{\mathrm{v}}_{\mathrm{FR}} = \sqrt{\mathrm{trace}\left(\mathbf{B}^{\mathrm{v}}_{\mathrm{FR}}\right)/3} \tag{11}$$

where $\mathbf{B}^{\mathrm{v}}_{\mathrm{FR}} = \mathbf{F}^{\mathrm{v}}_{\mathrm{FR}}\mathbf{F}^{\mathrm{v}^T}_{\mathrm{FR}}$ is the viscous left Cauchy-Green strain tensor.

Motivated by the reptational motion of FR chains, the Bergstrom-Boyce [35] power law is used to capture the nonlinear stretch-dependency as well as stress-dependency of the effective viscosity:

$$\dot{\gamma}_{\mathrm{FR}} = r\left|\lambda_{\mathrm{v}} - 1\right|^{-d}\left\|\boldsymbol{\sigma}_{\mathrm{FR}}\right\|^{m} \tag{12}$$

where r is a positive viscous multiplier parameter, d is the stretch-dependency parameter and m is the stress-dependency parameter.

In what follows, these general relations of the chains network physics are used to assess the aging effect on the relationship between macroscopic inelastic features of filled rubbers and the physically interpretable material constants (related to cross-linked chains and free chains) along with the amplified effect of the fillers.

2.2. Thermal aging mechanisms

Two types of aging are considered:

- **Intermittent relaxation:** The rubber is first thermally aged and the effect of aging on the relaxed response (at the end of the physical relaxation) and the inelastic response (hysteresis and physical relaxation) is then measured at room temperature (RT).
- **Continuous relaxation (or chemical relaxation):** The rubber is thermally aged while it is held in the stretched state.

In the following subsections, we present the constitutive theory for the two types of aging by considering the presence of inelastic effects. A novel approach is developed to take into account the coupling between inelasticity and network alteration induced by the thermal aging.

2.2.1. Thermal aging and intermittent relaxation

Thermal aging of rubbers consists in a complex reaction scheme which is not fully elucidated [1-4]. It may be, however, simply recognized that the material response evolution of thermally aged rubbers is essentially affected by chemical changes in the network structure. Cross-linking and chain scission are the two main competitive processes dependent on multi-factors, e.g. temperature, exposure time, material formulation (gum, fillers and antioxidants), etc. The evolution with aging of the two mechanisms is schematically depicted in Fig. 3. They have counterbalancing influences on the CL network: The cross-linking mechanism decreases the chain length whereas the scission mechanism decreases the chain density. The two competitive mechanisms occurring at the same time modify the average value of the chain density n_{CL} of the CL network. Its continuous evolution is proposed to be governed by an Arrhenius-type expression:

$$\dot{n}_{\mathrm{CL}} = \beta_{\mathrm{CL}} \left(n_{\mathrm{CL}} - n_{\mathrm{CL0}} \left(1 + \alpha_{\mathrm{CL}} \right) \right) \exp\left(\frac{E_a}{R} \left(\frac{1}{T} - \frac{1}{T_0} \right) \right) \tag{13}$$

in which the superposed dot denotes the exposure time derivative, $n_{\mathrm{CL}}\left(t=0\right) = n_{\mathrm{CL0}}$, E_a is the activation energy, α_{CL} and β_{CL} are two material constants, T is the aging temperature and R is the perfect gas constant. The exponential term corresponds to a shift factor noted a_T allowing to construct master curves (with T_0 an arbitrarily selected reference temperature). Cross-linking and chain scission are not distinguished. The total number of connected rigid-links in the CL network remaining constant during the network alteration, the chain-scale material kinetics (13) is restricted by the following relationship: $n_{\mathrm{CL}} N_{\mathrm{CL}} = n_{\mathrm{CL0}} N_{\mathrm{CL0}}$ in which n_{CL0} and N_{CL0} are the reference values associated to the unaged network.

In the present network alteration theory, CL chains and FR chains interact together as illustrated in Fig. 3. The motions of the FR chains can be significantly altered by any chemical changes of the CL network on which they are superimposed. This can be conceptually described using the Doi and Edwards [36] tube concept considering the reptational motion of an individual FR chain along the centerline of a tube-like region in which it is inserted due to CL chains or fillers from its neighborhood. The FR chains can only reptate (move back and forth) along the centerline of the tube-like region by reptational Brownian motion. The cross-linking (resp. chain scission) mechanism occurring in the CL network can effectively decrease (resp. increase) the reptational motion capability of an individual FR chain as a consequence of changes over time of the CL chains in the neighborhood of the individual FR chain which restrict (resp. enhance) its lateral motion. The higher the cross-linking (resp. chain scission) degree is, the higher (resp. smaller) the chain density in the CL network is. As a consequence, the cross-linking (resp. chain scission) mechanism leads to a smaller (resp. higher) tube diameter and a lower (resp. higher) mobility

of the FR chain. The objectively existing interaction between the CL and FR chains is introduced by considering that the viscous material constants of the FR chains are functions of the alteration kinetics of the CL network:

$$C_{\mathrm{FR}} = \hat{C}_{\mathrm{FR}}\left(n_{\mathrm{CL}}/n_{\mathrm{CL0}}\right),\ r = \hat{r}\left(n_{\mathrm{CL}}/n_{\mathrm{CL0}}\right),\ d = \hat{d}\left(n_{\mathrm{CL}}/n_{\mathrm{CL0}}\right) \text{ and } m = \hat{m}\left(n_{\mathrm{CL}}/n_{\mathrm{CL0}}\right) \tag{14}$$

Note that the parameter n_{CL} refers to chemical link density in the broad sense including inter-aggregates links and inter-chains cross-links. Indeed, fillers dispersed in the rubber gum may be regarded as junction points in the CL network acting as an amplifying factor in all elastic and viscous material constants [37-38] but also as amplifying factor of thermally activated alterations. The constitutive representation consists to regard the rubber-filler material system as a two-phase composite with infinitely stiff filler aggregates compared to the rubber gum, the two phases acting in parallel [17].

2.2.2. Continuous relaxation

While the material is held in the stretched state at the high temperature, that is, chemical relaxation, a portion of the whole CL network is altered by breakdown-rebound mechanisms of links (chemical inter-chains cross-links and inter-aggregates links) while another portion remains intact [8]. The CL network contains thus two superimposed sub-networks acting in parallel: the original CL network and the newly born CL network. The Cauchy stress $\boldsymbol{\sigma}_{\mathrm{CL}}$ of the whole CL network becomes additively split into two subparts:

$$\boldsymbol{\sigma}_{\mathrm{CL}} = \boldsymbol{\sigma}_{\mathrm{CL\_1}} + \boldsymbol{\sigma}_{\mathrm{CL\_2}} \tag{15}$$

We refer by the subscripts 1 and 2, respectively, the original network and the newly born network. The two CL networks have respective average chain densities $n_{\mathrm{CL\_1}}$ and $n_{\mathrm{CL\_2}}$, and average chain lengths $N_{\mathrm{CL\_1}}$ and $N_{\mathrm{CL\_2}}$.

Because the original CL network is at equilibrium when the material is un-stretched while the newly formed CL network is at equilibrium when the material is stretched (i.e. stress-free at the moment of the rebound), the kinematics must be specified. The two CL networks have thus distinct reference configurations. The mapping of a material point in the portion of the CL network still having the original CL network is described using the deformation gradient:

$$\mathbf{F}_{\mathrm{CL}}\left(t,t_0\right)=\partial \boldsymbol{x}_t/\partial \boldsymbol{X}_{t_0} \tag{16}$$

in which $\boldsymbol{X}_{t_0}$ is the initial position at time t_0 (in configuration Ω_{t_0}) and $\boldsymbol{x}_t$ is the current position at time t (in configuration Ω_t). The mapping of a material point in the portion of the CL network having the newly formed CL network requires the introduction of an intermediate (relaxed) configuration Ω_τ at a time τ in which the material point has the position $\boldsymbol{x}_\tau$. Using this conceptual sequence of configurations, the deformation gradient $\mathbf{F}_{\mathrm{CL}}\left(t,t_0\right)$ takes thus a multiplicative form:

$$\mathbf{F}_{\mathrm{CL}}\left(t,t_0\right)=\mathbf{F}_{\mathrm{CL}}\left(t,\tau\right)\mathbf{F}_{\mathrm{CL}}\left(\tau,t_0\right) \tag{17}$$

in which two successive arrangements are considered:

$$\mathbf{F}_{\mathrm{CL}}\left(t,\tau\right)=\partial \boldsymbol{x}_t/\partial \boldsymbol{x}_\tau \text{ and } \mathbf{F}_{\mathrm{CL}}\left(\tau,t_0\right)=\partial \boldsymbol{x}_\tau/\partial \boldsymbol{X}_{t_0} \tag{18}$$

Remind that the newly formed network is stress-free at the instant τ of its nucleation and it does not contribute to the chemical stress:

$$\boldsymbol{\sigma}_{\mathrm{CL\_2}}=\mathbf{0} \text{ and } \mathbf{F}\left(\tau,\tau\right)=\mathbf{I} \tag{19}$$

When the material is held in the stretched state at the high temperature, the total stress is thus:

$$\boldsymbol{\sigma}_{\mathrm{CL}}=\boldsymbol{\sigma}_{\mathrm{CL\_1}} \tag{20}$$

Macroscopically manisfested by a permanent deformation (this plastic-like deformation being an important insight of the permanent molecular alteration), the second network tends to maintain the specimen in its stretched state because at the moment of its nucleation τ it is at

its equilibrium state. The stress-free condition of the CL network, when the chemical relaxation is interrupted, implies the following condition:

$$\boldsymbol{\sigma}_{\mathrm{CL}} = \mathbf{0} \text{ and } \mathbf{F}_{\mathrm{CL}}\left(t, t_0\right) = \mathbf{F}^{\mathrm{p}} \tag{21}$$

in which the superscrip p denotes the deformation in the frozen state (permanent deformation) after mechanical unload.

A quantitative evaluation of the permanent deformation $\mathbf{F}^{\mathrm{p}}$ can be thus obtained from the resolution of the following formula:

$$\boldsymbol{\sigma}_{\mathrm{CL\_1}}\left(\mathbf{F}^{\mathrm{p}}\right) + \boldsymbol{\sigma}_{\mathrm{CL\_2}}\left(\mathbf{F}^{\mathrm{p}}\mathbf{F}^{-1}\right) = \mathbf{0} \tag{22}$$

where $\mathbf{F} = \mathbf{F}_{\mathrm{CL}}\left(\tau, t_0\right)$ is the deformation of the original network while it is held in the stretched state at the high temperature. Eqs. (6) and (8) are used in the relation (22) in which the respective physical-related quantities of the two networks are introduced. In our approach, the relaxed response at RT of previously aged rubber (having undergone continuous relaxation at high temperature) allows to obtain the aging-induced evolution of the overall CL network properties considering the formulation of the previous section, and then that of the newly formed CL network properties. The consistent representation of the CL network evolution is ensured by the conservation law: The total number of connected rigid-links in the CL network remains constant during second network formation. That is to say that the increase in average chain density with aging results in a decrease in the average number of connected rigid-links in a chain. Note that links are broken and reformed at the same time τ for creating the second CL network in the stretched state. The modification of mobility of the FR chains due to reformation of broken links is taken into account by considering the aging-induced changes in movements of the FR chains as a direct consequence of the degradation of the CL network. In our approach, the rubber relaxation is thus caused by two concomitant mechanisms: scission mechanism of CL chains and viscoelastic mechanism of FR chains. Although being

recoverable [39], the amount of the viscous stretch of the FR network obtained when the material is mechanically unloaded (remanent strain observed at zero stress) can be taken as an additional effect in the (apparent) plastic-like deformation.

The next section presents an experimental investigation of aging effects on the time-dependent material response of a rubber-filler material system exposed in air at high temperatures.

3. Application to carbon-filled SBR

3.1. Experiments

A sulfur-vulcanized styrene-butadiene rubber (SBR) is used to illustrate the proposed approach. This is an industrial material, supplied by Trelleborg Group, which contains stabilizers to decrease the aging rate and various amounts of N330 carbon-black. The rubber mixtures were vulcanized by compression molding method. Table 1 lists the compound formulation. The material is a rubber-filler system filled with 15 phr, 25 phr and 43 phr (per hundred rubber, in weight) parts of carbon-black and will be referred to as SBR15, SBR25 and SBR43, respectively. The values of 15 phr, 25 phr and 43 phr correspond to a carbon-black volume fraction v_f of 9.16 %, 14.39 % and 22.42 %, respectively. Dog-bone shaped specimens, with gauge dimensions of 25 mm (length) × 4 mm (width) × 2 mm (thickness), were cut from SBR sheets. Fig. 4 provides an illustration of the two-step loading condition: the chemical relaxation (first step) is followed by a physical relaxation (second step) in a loading-unloading cycle:

- **Chemical relaxation:** A dedicated set-up was designed in order to uniformly expose the specimens to high temperatures in the air-ventilated oven. The specimens were isothermally aged at 383°K, 403°K and 423°K for various exposure times t as illustrated in Fig. 4a. While the samples were aged, they were held at a true strain of

50% in order to provoke a chemical relaxation. The specimens, previously aged, were mechanically unloaded and cooled down to RT by natural cooling. The final specimen length, intermediate between the initial specimen length and the stretched length, was measured. The true axial plastic-like deformation is then determined for different conditions in terms of aging temperature T and exposure time t. The measurements were repeated at least three times.

- **Physical relaxation:** The consequences of the thermal aging on the material behavior were examined at RT. After aging and come back to RT, the specimens were then submitted to multi-step (physical) stress relaxation under a loading-unloading cycle at RT using an electro-pulse testing machine Instron-5500. The true (axial and transversal) strains were monitored by a videomeasurement technique (The details can be found elsewhere [31]) and the applied load, simultaneously recorded by the testing machine load-cell, was converted into true axial stress. The same absolute axial true strain rate of 0.001 /s was imposed to the loading and unloading segments. At three prescribed strain levels, physical relaxation periods with a holding time of 1 h were applied to each segment. Each mechanical test was performed on a newly aged specimen in terms of aging temperature T and exposure time t. The continuous evolution in micro-structural parameters (Eqs. (13) and (14)) is then extracted from the obtained multi-step stress relaxation responses at RT.

3.2. General observations

Fig. 5 reports the responses of the thermally aged materials for different durations at 383°K, 403°K and 423°K, respectively. We first focus on the experimental results plotted as solid lines. A global view at these curves shows that the thermal aging affects significantly both the stabilized relaxed-stress (approached in long-term physical stress relaxation) and the

hysteretic behavior (see also the unaged response in Fig. 1). Moreover, the stress evolution during the physical relaxation periods in the loading segment can be seen severely affected by the thermal aging whereas the effects on the unloading segment seem to be much less pronounced. Comparing the stress limits at the end of the relaxation periods, the data show a stiffening of the equilibrium material response with increasing exposure time. This observation confirms that the dominant degradation mechanism is cross-linking process which leads over the exposure time to increase the level of interactions between the two populations of chains, that is, CL and FR chains, while increasing the aging temperature accelerates this process. As a consequence, the hysteresis loop exhibits an increase in its area with aging. Due to the presence of inter-aggregates links, the total number of links increases with the filler content and amplifies the effect of aging on all macro-observations including physical relaxation, hysteresis and plastic-like deformation.

3.3. Model fit and material kinetics

The experimental observations illustrate the complexity of the aging-induced material response evolution regarding especially the inelastic effects. Using our simple network decomposition, the aim is to design the material kinetics in order to capture the general trend of the time-dependent rubber response. Inherent to the model structure, the CL chains parameters and the FR chains parameters can be identified separately. The parameters of the two kinds of chains are treated as constants at each exposure time of a given aging temperature and, the material kinetics is then deduced.

3.3.1. CL chains parameters

The CL chains parameters are determined from the nonlinear equilibrium response deduced from the multi-step stress relaxation. The static stiffness $C_{\mathrm{CL}} = n_{\mathrm{CL}} k_{\mathrm{B}} T$ may be extracted from the following formula:

$$C_{\mathrm{CL}} = 3\sigma_{\mathrm{CL}} \left\{ \frac{\sqrt{N_{\mathrm{CL}}}}{\lambda_{\mathrm{CL}}} \mathrm{L}^{-1}\left(\frac{\lambda_{\mathrm{CL}}}{\sqrt{N_{\mathrm{CL}}}} \right) \left(\lambda^2 - \frac{1}{\lambda} \right) \right\}^{-1} \tag{23}$$

where σ_{CL} is the uniaxial Cauchy stress of the nonlinear equilibrium curve and λ is the uniaxial stretch.

The value of N_{CL} can be further determined by considering that the denominator of the Padé approximation given by Eq. (7) is equal to zero:

$$N_{\mathrm{CL}} = \frac{1}{3}\left(\lambda_{\infty}^2 + \frac{2}{\lambda_{\infty}} \right) \tag{24}$$

in which λ_{∞} is the uniaxial stretch for which the stress increases in an exponential way.

The CL chains parameters of the unaged materials, n_{CL0} and N_{CL0}, are given in Table 2. The identification is then performed for each aging condition. Fig. 6 gives the evolution of $n_{\mathrm{CL}}/n_{\mathrm{CL0}}$ for the three materials. Recall that the conservation law implies that $N_{\mathrm{CL0}}/N_{\mathrm{CL}} = n_{\mathrm{CL}}/n_{\mathrm{CL0}}$. Fig. 6 allows following the impact of the thermal aging on the network structure. As expected, increasing the exposure time leads to the increase of the average CL chain density (and thus to the decrease of the average CL chain length). This evolution is dramatically amplified by increasing the aging temperature, but the data are aggregated thanks to the shift factor a_T (the reference temperature T_0 is taken equal to 403 K). Several experimental works show that during thermal aging the dispersed carbon-black fillers agglomerate to form a filler network across the rubber gum [5, 40-42]. Note that the average CL chain density kinetics includes the cross-linking mechanism of CL chains but also the

bounding mechanism of inter-aggregates links. The alteration kinetics of the CL network is fitted using the formula (13) and the related parameters are given in Table 2.

3.3.2. FR chains parameters

The FR chains parameters are determined from the time-dependent deviation from equilibrium. The viscous stiffness C_{FR} is determined using the tangent modulus of the instantaneous unloading $E_{\mathrm{u}} = d\sigma/d\varepsilon$ of the multi-step stress relaxation and the static stiffness $C_{\mathrm{CL}}\left(2\lambda_u^2 + 1/\lambda_u\right)/3$ at the uniaxial stretch reversal λ_u:

$$C_{\mathrm{FR}} = E_u - \frac{C_{\mathrm{CL}}}{3}\left(2\lambda_u^2 + \frac{1}{\lambda_u}\right) \tag{25}$$

Because the loading and unloading paths are differently affected by the thermal aging, a slight modification is brought to the formula (12) by postulating that the motion of the superimposed FR chains differs between a mechanical loading and a mechanical unloading. This is done by assuming a differentiation between loading path and unloading path, the related parameters being denoted by the subscripts l and u, respectively. They were obtained through the adjustment of the best relaxation and hysteretic responses by means of trial and error. The values of the unaged materials are provided in Table 2 and the comparison with the experimental data can be observed in Fig. 1. Due to the interdependence of certain inelastic parameters [33], a special care was done on the identification of the FR chains parameters in order to obtain monotonic evolutions with variation in aging temperature, exposure time and filler content. The results are plotted in Figs. 7-9 and can be fitted by the following expression:

$$\mathrm{FR}/\mathrm{FR}_0 = 1 + \alpha_{\mathrm{FR}}\left(1 - \exp\left(\beta_{\mathrm{FR}} t a_T\right)\right) \tag{26}$$

where α_{FR} and β_{FR} are two fitting coefficients and, FR_0 is the initial value of the FR parameter.

The capability of the constitutive model to adequately capture the important features of the observed material response is shown in Fig. 5 for aging temperatures of 383°K, 403°K and 423°K. The correlation of the model with the experimental data can be considered as acceptable and in some cases very good, over the range of investigated aging temperatures. In particular, the model capability to catch the evolutions in stiffness, hysteresis amount, associated overstress and remanent strain (observed at zero stress) is remarkably good. It is also very satisfying to observe that the reproduction quality of the model also applies to the aging temperature which was not used in the material kinetics design. The rate-dependence is obviously affected by the aging as observed in the illustrative examples provided in Fig. 10. The comparison with experimental data of aged materials loaded at different strain rates will be needed to further verify the model and the related identification.

The increase of the FR chain viscosity parameter C_{FR} with aging time translates the increase of the overall material viscoelastic damping as evidenced by the hysteresis area increase. In the meantime, the creation of new chemical links (between filler aggregates and between elastically active CL chains) decreases the mobility of FR chains. The proposed network alteration theory can be interpreted via the tube concept: new chemical links can effectively restrict the lateral motion of an individual FR chain into the tube-like region. Thus, the tube diameter decreases with aging time as evidenced by the evolutions of the parameters r_l and r_u. The latter parameters, describing the rates of relaxation, exhibit similar evolutions. That is to say that the time to return to a more relaxed configuration is equivalent upon loading and unloading paths. Nonetheless, the aging affects the nonlinear history-dependency and, different strain and stress dependencies of reptational dynamics of FR chains are found under stretching and recovery. Indeed, the stretch-dependency parameter d was found independent

on aging under loading, i.e. $d_l = d_{l0}$, while it increases with aging time under unloading. The stress-dependency parameter m decreases and increases with aging time under loading and unloading, respectively.

3.3. Aging effect on CL and FR chains interactions

As mentioned above, the material degradation in our network alteration theory is assumed to be strictly linked to the evolution of the average CL chain density. The FR chain material constants can be thus directly related to average CL chain density. In the meantime, due to the amplifying effect of the fillers, the inelastic response of the aged rubber-filler system is strongly dependent on the filler content. The FR chains parameters are plotted in Fig. 11 as a function of the CL chains parameters such that straight lines are obtained. Linear dependency of the fracture properties with the average molar mass of elastically active chains is classically reported for thermally aged rubbers [7, 43]. Quite interestingly, we obtain also linear dependencies with the viscous material constants describing the FR chains features. The lines of Fig. 11 can be fitted by linear laws with slopes A_{FR}:

$$\mathrm{FR} = \mathrm{FR}_0 + A_{\mathrm{FR}}\mathrm{FR}_0\left(n_{\mathrm{CL}}/n_{\mathrm{CL0}} - 1\right) \tag{24}$$

in which the constants are provided in Table 2 for the three materials.

It is worth noticing that the abscissa axis of Fig. 11 indicates the alteration of the CL network including the effects of aging temperature, exposure time and filler content at the same time. All the slopes, in absolute value, decrease with increasing filler content. The latter reflect the level of interactions between the FR chains and the CL network, including CL chains and fillers acting as junction points in the CL network. Note that the level of interactions means the level of mobility of the FR chains.

3.4. Model prediction

In this section, we come back to the aging process undergone by the materials. It consists to a thermal aging in the stretched state, that is, chemical relaxation. Remind that the above material kinetics was designed after chemical relaxation treatment. It would be thus interesting to implement them in the constitutive theory in order to predict the response upon chemical relaxation. Indeed, such predictions are fundamental for many technical applications, such as rubber seals and rubber connectors, that are pre-strained at elevated temperatures and for which the loss of pressure is undesirable and may impact the operational life.

Figs. 12 and 13 present the model predictions in terms of plastic-like deformation and stress response over a period of reduced exposure time for the different filler concentrations. These material responses allow estimating these two quantities for an aging temperature or an exposure time (not experimentally measured) by extrapolation. Fig. 12 shows that the model underestimates the experimental observations when it considers only the permanent microstructure change induced by the newly born network. Nonetheless, when the additional effect of the remanent strain induced by the presence of FR chains is taken into account, the model is able to remarkably predict the plastic deformation. Note that the additional remanent strain, retained in the material when the mechanical loading is removed, can be recovered but it necessitates a very long recovery time that is not assessed in the present work. Fig. 13 shows how the alteration mechanisms affect the stress decay. The irreversible loss of connectivity of CL chains due to scission leads to a continuous stress decay that is proportional to the change in chemical link density sustaining it and depends via the designed kinetics on aging temperature, exposure time and filler content. The stress is decaying more rapidly when physical relaxation effects due to rearrangement of FR chains and chemical relaxation effects are considered at the same time. The time to which the overall stress approaches to zero depends strongly on aging temperature, exposure time and filler content.

The model results demonstrate the importance of the inelastic effects on the prediction of long-term material response due to thermally activated degradation.

The proposed constitutive model seems to be a promising tool to simulate continuous relaxation of rubber at high temperature. Nonetheless, the aging that rubber undergoes is almost always in an environment with oxygen [44]. The aging was assumed here homogeneous through the transverse direction, i.e. the oxygen distribution through the thickness is such that the aging process is not limited by oxygen diffusion and oxidation due to oxygen is homogeneous (what is reasonable for a thickness of 2 mm according to [45-46]). However, the proposed tool should be enriched for thick structures in regards to the surface versus bulk network degradation [47]. The degradation should be then regarded as a heterogeneous oxidative process due to oxygen diffusion/consumption through the material [48-49]. Indeed, diffusion-limited oxidation within the material results in the appearance of an oxidized layer depending on aging temperature, exposure time, compound formulation (fillers, antioxidants, oxygen permeability, etc.) and sample thickness [50-51]. This limitation deserves to be the subject of a next model evolution.

4. Concluding remarks

In this contribution, we derived a novel time-dependent constitutive model for the prediction of the inelastic response of thermally aged rubbers in connection to the collection of chemical and physical changes. Using an accelerated aging procedure and the time-temperature equivalence principle for a SBR containing different amounts of carbon-black fillers, the master curves of the material kinetics were designed as a function of a reduced time as well for the CL chain network as for the FR chain network. The implications of the chemically induced unrecoverable alterations of the CL network on the recoverable physical mechanisms of the FR network were highlighted.

A complete verification of the proposed approach considering more complex loading conditions remains an important issue for future works. The incorporation of the thermo-oxidative aging in our approach remains also an important issue for thick structures in the aim to predict the heterogeneous molecular alterations in terms of scission/rebound mechanism of CL chains and recoverable motion of FR chains which should be governed by chemical reaction rates.

Acknowledgments
This work was financially supported by the Shandong Province Special Grant for High-Level Overseas Talents and the research fund of Shandong Academy of Sciences (Grant No. 2017QN001, 2019GHPY11 and KJHZ201805).

References

[1] Colin, X., Audouin, L., Verdu, J., 2007. Thermal oxidation kinetics of unvulcanized unstabilized polyisoprene. Rubber Chemistry and Technology 80, 621-641.
[2] Le Gac, P.Y., Celina, M., Roux, G., Verdu, J., Davies, P., Fayolle, B., 2016. Predictive ageing of elastomers: oxidation driven modulus changes for polychloroprene. Polymer Degradation and Stability 130, 348-355.
[3] Luo, K., Ye, X., Zhang, H., Liu, J., Luo, Y., Zhu, J., Wu, S., 2020. Vulcanization and antioxidation effects of accelerator modified antioxidant in styrene-butadiene rubber: Experimental and computational studies. Polymer Degradation and Stability 177, 109181.
[4] Mohammadi, H., Morovati, V., Poshtan, E., Dargazany, R., 2020. Understanding decay functions and their contribution in modeling of thermal-induced aging of cross-linked polymers. Polymer Degradation and Stability 175, 109108.
[5] Schwartz, G.A., Cerveny, S., Marzocca, A.J., Gerspacher, M., Nikiel, L., 2003. Thermal aging of carbon black filled rubber compounds. I. Experimental evidence for bridging flocculation. Polymer 44, 7229-7240.
[6] Colin, X., Audouin, L., Verdu, J., 2007b. Kinetic modelling of the thermal oxidation of polyisoprene elastomers. Part III- Oxidation induced changes of elastic properties. Polymer Degradation and Stability 92, 906-914.
[7] Ben Hassine, M., Naït-Abdelaziz, M., Zaïri, F., Colin, X., Tourcher, C. and Marque, G., 2014. Time to failure prediction in rubber components subjected to thermal ageing: A combined approach based upon the intrinsic defect concept and the fracture mechanics. Mechanics of Materials 79, 15-24.
[8] Tobolsky, A.V., Takahashi, Y., Naganuma, S., 1972. Effect of additional cross-linking of continuous chemical stress relaxation of cis-Polybutadiene. Polymer Journal 3, 60-66.
[9] Chinn, S., DeTeresa, S., Sawvel, A., Shields, A., Balazs, B., Maxwell, R.S., 2006. Chemical origins of permanent set in a peroxide cured filled silicone elastomer - tensile and ^{1}H NMR analysis. Polymer Degradation and Stability 91, 555-564.
[10] Mott, P.H., Roland, C.M., 2000. Mechanical and optical behavior of double network rubbers. Macromolecules 33, 4132-4137.
[11] Singh, N.K., Lesser, A.J., 2010. Mechanical and thermo-mechanical studies of double networks based on thermoplastic elastomers. Journal of Polymer Science: Part B: Polymer Physics 48, 778-789.

[12] Wang, W., Zhang, Z., Theodoros, D., Liu, J., Gao, Y., Zhang, L., Lyulin, A.V., 2017. Simulational insights into the mechanical response of prestretched double-network filled elastomers. Soft Matter 13, 8597-8608.
[13] Rottach, D.R., Curro, J.G., Grest, G.S., Thompson, A.P., 2004. Effect of strain history on stress and permanent set in cross-linking networks: A molecular dynamics simulations. Macromolecules 37, 5468-5473.
[14] Rottach, D.R., Curro, J.G., Budzien, J., Grest, G.S., Svaneborg, C., Everaers, R., 2006. Permanent set of cross-linking networks: Comparison of theory with molecular dynamics simulations. Macromolecules 39, 5521-5530.
[15] Neuhaus, C., Lion, A., Johlitz, M., Heuler, P., Barkhoff, M., Duisen F., 2017. Fatigue behavior of an elastomer under consideration of ageing effects. International Journal of Fatigue 104, 72-80.
[16] Guo, Q., Zaïri, F., Guo, X., 2018. A thermo-viscoelastic-damage constitutive model for cyclically loaded rubbers. Part I: Model formulation and numerical examples. International Journal of Plasticity 101, 106-124.
[17] Guo, Q., Zaïri, F., Guo, X., 2018. A thermo-viscoelastic-damage constitutive model for cyclically loaded rubbers. Part II: Experimental studies and parameter identification. International Journal of Plasticity 101, 58-73.
[18] Ayoub, G., Naït-Abdelaziz, M., Zaïri, F., Gloaguen, J.M., Charrier, P., 2012. Fatigue life prediction of rubber-like materials under multiaxial loading using a continuum damage mechanics approach: Effects of two-blocks loading and R ratio. Mechanics of Materials 52, 87-102.
[19] Septanika, E.G., Ernst, L.J., 1998. Application of the network alteration theory for modeling the time-dependent constitutive behaviour of rubbers. Part II. Further evaluation of the general theory and experimental verification. Mechanics of Materials 30, 265-273.
[20] Shaw, J.A., Jones, A.S., Wineman, A.S., 2005. Chemorheological response of elastomers at elevated temperatures: Experiments and simulations. Journal of the Mechanics and Physics of Solids 53, 2758-2793.
[21] Belbachir, S., Zaïri, F., Ayoub, G., Maschke, U., Naït-Abdelaziz, M., Gloaguen, J.M., Benguediab, M., Lefebvre, J.M., 2010. Modelling of photodegradation effect on elastic-viscoplastic behaviour of amorphous polylactic acid films. Journal of the Mechanics and Physics of Solids 58, 241-255.
[22] Johlitz, M., 2012. On the representation of ageing phenomena. The Journal of Adhesion 88, 620-648.
[23] Steinke, L., Spreckels, J., Flamm, M., Celina, M., 2011. Model for heterogeneous aging of rubber products. Plastics, Rubber and Composites 40, 175-179.
[24] Johlitz, M., Diercks, N., Lion, A., 2014. Thermo-oxidative ageing of elastomers: a modelling approach based on a finite strain theory. International Journal of Plasticity 63, 138-151.
[25] Bouaziz, R., Ahose, K.D., Lejeunes, S., Eyheramendy, D., Sosson, F., 2019. Characterization and modeling of filled rubber submitted to thermal aging. International Journal of Solids and Structures 169, 122-140.
[26] Mohammadi, H., Dargazany, R., 2019. A micro-mechanical approach to model thermal induced aging in elastomers. International Journal of Plasticity 118, 1-16.
[27] Wineman, A., Shaw, J., 2019. Coupled thermal- and deformation-induced degradation in planar rubber membranes under radial loading. Mathematics and Mechanics of Solids 24, 3103-3124.
[28] Zhi, J., Wang, Q., Zhang, M., Zhou, Z., Liu, A., Jia, Y., 2019. Coupled analysis on hyper-viscoelastic mechanical behavior and macromolecular network alteration of rubber during thermo-oxidative aging process. Polymer 171, 15-24.

[29] Bahrololoumi, A., Morovati, V., Poshtan, E.A., Dargazany, R., 2020. A multi-physics constitutive model to predict hydrolytic aging in quasi-static behaviour of thin cross-linked polymers. International Journal of Plasticity 130, 102676.
[30] Aït-Hocine, N., Hamdi, A., Naït-Abdelaziz, M., Heuillet, P., Zaïri, F., 2011. Experimental and finite element investigation of void nucleation in rubber-like materials. International Journal of Solids and Structures 48, 1248-1254.
[31] Zaïri, F., Naït Abdelaziz, M., Gloaguen, J.M., Lefebvre, J.M., 2011. A physically-based constitutive model for anisotropic damage in rubber-toughened glassy polymers during finite deformation. International Journal of Plasticity 27, 25-51.
[32] Arruda, E.M., Boyce, M.C., 1993. A three-dimensional constitutive model for the large stretch behavior of rubber elastic materials. Journal of the Mechanics and Physics of Solids 41, 389-412.
[33] Pyrz, M., Zaïri, F., 2007. Identification of viscoplastic parameters of phenomenological constitutive equations for polymers by deterministic and evolutionary approach. Modelling and Simulation in Materials Science and Engineering 15, 85-103.
[34] Zaïri, F., Woznica, K., Naït-Abdelaziz, M., 2005. Phenomenological nonlinear modelling of glassy polymers. Comptes Rendus Mecanique 333, 359-364.
[35] Bergstrom, J.S., Boyce, M.C., 1998. Constitutive modeling of the large strain time-dependent behavior of elastomers. Journal of the Mechanics and Physics of Solids 46, 931-954.
[36] Doi, M., Edwards, M.F., 1986. The Theory of Polymer Dynamics. Oxford University Press, Oxford.
[37] Ovalle-Rodas, C., Zaïri, F., Naït-Abdelaziz, M., Charrier, P., 2015. Temperature and filler effects on the relaxed response of filled rubbers: experimental observations on a carbon-filled SBR and constitutive modeling. International Journal of Solids and Structures 58, 309-321.
[38] Ovalle-Rodas, C., Zaïri, F., Naït-Abdelaziz, M., Charrier, P., 2016. A thermo-visco-hyperelastic model for the heat build-up during low-cycle fatigue of filled rubbers: Formulation, implementation and experimental verification. International Journal of Plasticity 79, 217-236.
[39] Cherief, M.N.D., Zaïri, F., Ding, N., Gloaguen, J.M., Naït-Abdelaziz, M., Benguediab, M., 2020. Plasticity and thermally-induced recovery in polycarbonate. Mechanics of Materials 148, 103515.
[40] Azura, A.R., Ghazali, S., Mariatti, M., 2008. Effects of the filler loading and aging time on the mechanical and electrical conductivity properties of carbon black filled natural rubber. Journal of Applied Polymer Science 110, 747-752.
[41] Jovanovic, S.S, Jovanovic, V., Markovic, G., Cincovic, M.M, 2009. The effect of different types of carbon blacks on the rheological and thermal properties of acrylonitrile butadiene rubber. Journal of Thermal Analysis and Calorimetry 98, 275-283.
[42] He, S., Bai, F., Liu, S., Ma, H., Hu, J., Chen, L., Lin, J., Wei, G., Du, X., 2017. Aging properties of styrene-butadiene rubber nanocomposites filled with carbon black and rectorite. Polymer testing 64, 92-100.
[43] Lake, G.J., Thomas, A.G., 1967. The strength of highly elastic materials. Proceedings of the Royal Society Series A 300, 108-119.
[44] Mott, P.H., Roland, C.M., 2001. Aging of natural rubber in air and seawater. Rubber Chemistry and Technology 74, 79-88.
[45] Rincon-Rubio, L.M., Colin, X., Audouin, L., Verdu, J., 2003. A theoretical model for diffusion-limited thermal oxidation of elastomers at medium temperatures. Rubber Chemistry and Technology 76, 460-482.

[46] He, S.J., Wang, Y.Q., Xi a, M.M., Lin, J., Xue, Y., Zhang, L.Q., 2013. Prevention of oxide aging acceleration by nano-dispersed clay in styrene-butadiene rubber matrix. Polymer Degradation and Stability 98, 1773-1779.
[47] Guo, Q., Zaïri, F., Ovalle-Rodas, C., Guo, X., 2018. Constitutive modeling of the cyclic dissipation in thin and thick rubber specimens. Journal of Applied Mathematics and Mechanics 98, 1878-1899.
[48] Moon, B., Jun N., Park, S., Seok, CS, Hong, US. 2019. A study on the modified Arrhenius equation using the oxygen permeation block model of crosslink structure. Polymers 11, 136.
[49] Dinari, A., Zaïri, F., Chaabane, M., Ismail, J., Benameur, T., 2021. Thermo-oxidative stress relaxation in carbon-filled SBR. Plastics, Rubber and Composites.
[50] Wise, J., Gillen, K.T., Clough, R.L., 1997. Quantitative model for the time development of diffusion-limited oxidation profiles. Polymer 38, 1929-1944.
[51] Quintana, A., Celina, M.C., 2018. Overview of DLO modeling and approaches to predict heterogeneous oxidative polymer degradation. Polymer Degradation and Stability 149, 173-191.

	SBR15	SBR25	SBR43
SBR	100	100	100
Carbon-black	15	25	43
Processing oil	37.5	37.5	37.5
Sulfur	3	3	3
Antioxidant	5.5	5.5	5.5
Zinc oxide	5	5	5
Accelerators	4	4	4
Stearic acid	3	3	3

Table 1. Compound formulation (value in phr, in weight).

Parameter	Unit	Significance	SBR15	SBR25	SBR43
n_{CL0}	[m^3]	Initial CL chain density	$7.365\times10^{+19}$	$8.838\times10^{+19}$	$1.227\times10^{+20}$
N_{CL0}		Initial CL chain length	57	55	40
C_{FR0}	MPa	Initial FR chain viscosity	0.3	0.36	1.5
r_{l0}	$\mathrm{MPa^{-1}\ s^{-1}}$	Initial viscous multiplier in load	0.1	0.09	0.01
d_{l0}		Initial stretch-dependency in load	1.5	1.7	1.7
m_{l0}		Initial stress-dependency in load	3.7	5.5	5.5
r_{u0}	$\mathrm{MPa^{-1}\ s^{-1}}$	Initial viscous multiplier in unload	1.7	0.99	0.9
d_{u0}		Initial stretch-dependency in unload	0.8	1.0	1.0
m_{u0}		Initial stress-dependency in unload	3.0	3.0	5.0
E_a	$\mathrm{kJ\ mol^{-1}}$	Activation energy	33.13	37.97	45.23
α_{CL}		Aging kinetics of CL chain density	1.74	2.86	3.98
β_{CL}		Aging kinetics of CL chain density	-1.02×10^{-2}	-1.05×10^{-2}	-1.71×10^{-2}
$A_{\mathrm{FR}}^{C_{\mathrm{FR}}}$		Aging kinetics of C_{FR}	3.01	2.77	2.55
$A_{\mathrm{FR}}^{r_l}$		Aging kinetics of r_l	-0.67	-0.41	-0.26
$A_{\mathrm{FR}}^{d_l}$		Aging kinetics of d_l	0	0	0
$A_{\mathrm{FR}}^{m_l}$		Aging kinetics of m_l	-0.44	-0.18	-0.07
$A_{\mathrm{FR}}^{r_u}$		Aging kinetics of r_u	-2×10^{-2}	-5×10^{-3}	-7×10^{-5}
$A_{\mathrm{FR}}^{d_u}$		Aging kinetics of d_u	1.73	0.75	0.42
$A_{\mathrm{FR}}^{m_u}$		Aging kinetics of m_u	1.04	0.9	0.79

Table 2. Model constants.

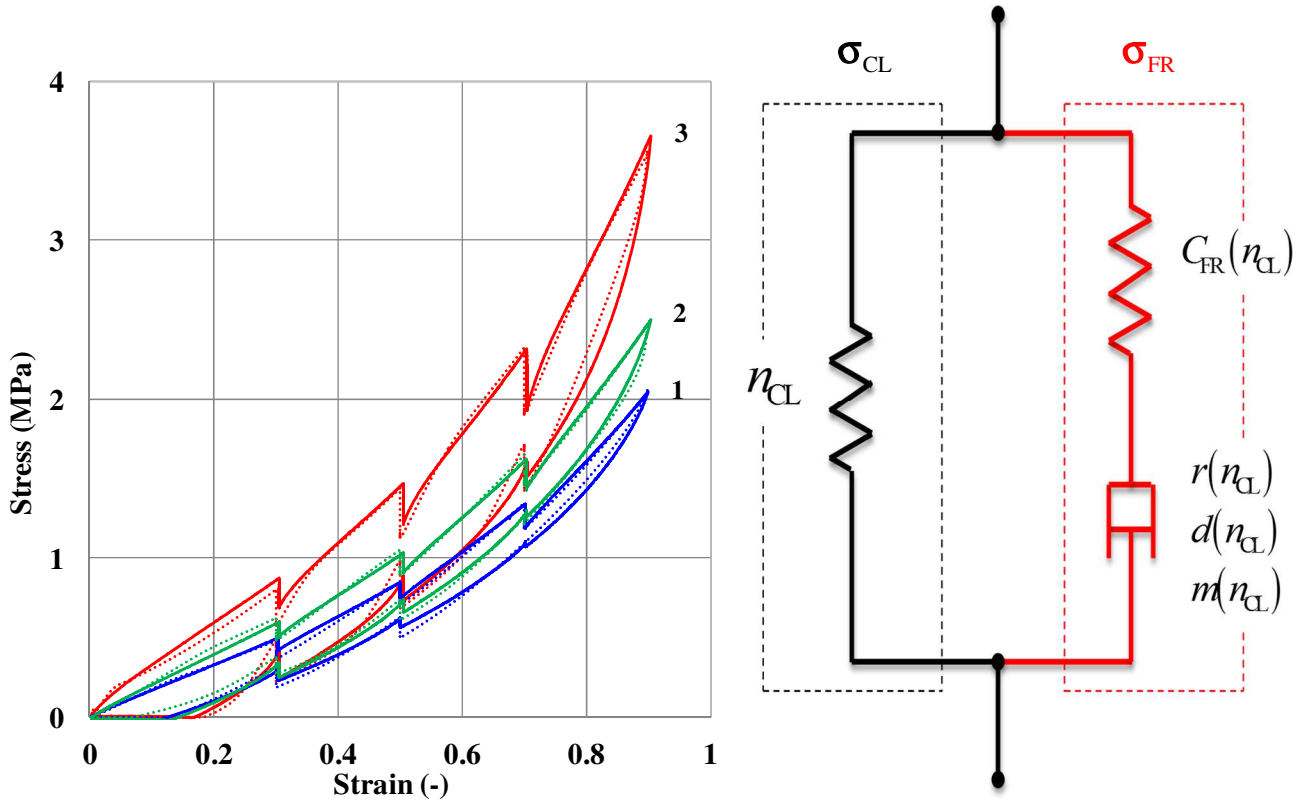

Figure 1. Multi-step stress relaxation responses at RT (solid lines: experiments, dashed lines: model) of unaged SBR (1: SBR15, 2: SBR25, 3: SBR43) and one-dimensional visualization analog of the rubber deformation model; the two branches, acting in parallel, are related to the CL chains (nonlinear elastic spring) and the FR chains (nonlinear elastic spring in series with viscous damper) whose parameters become coordinated.

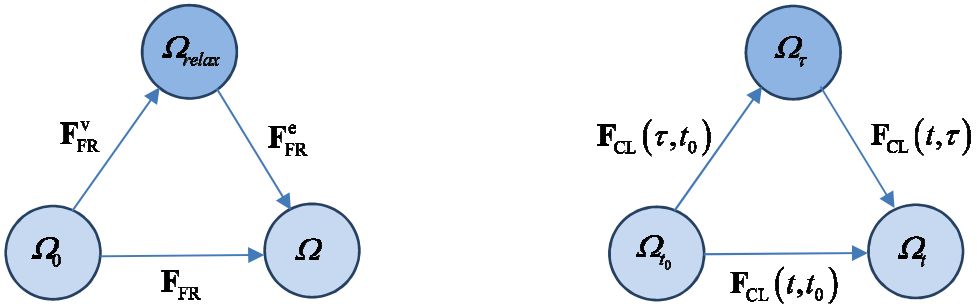

(a) (b)

Figure 2. Multiplicative decomposition of deformation for (a) physical relaxation of FR chains and (b) chemical relaxation of CL chains.

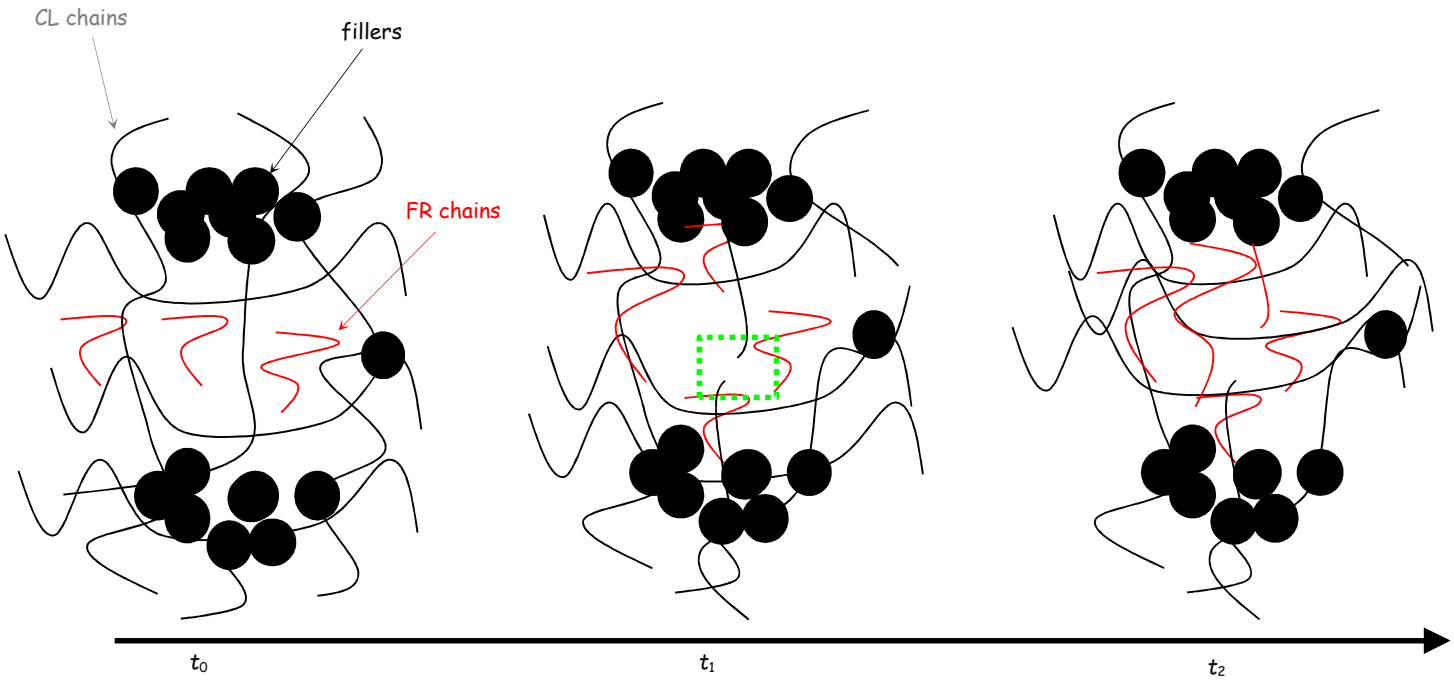

Figure 3. Evolution of the network structure during aging implying scission/cross-linking of CL network and leading to increasing FR-CL interactions.

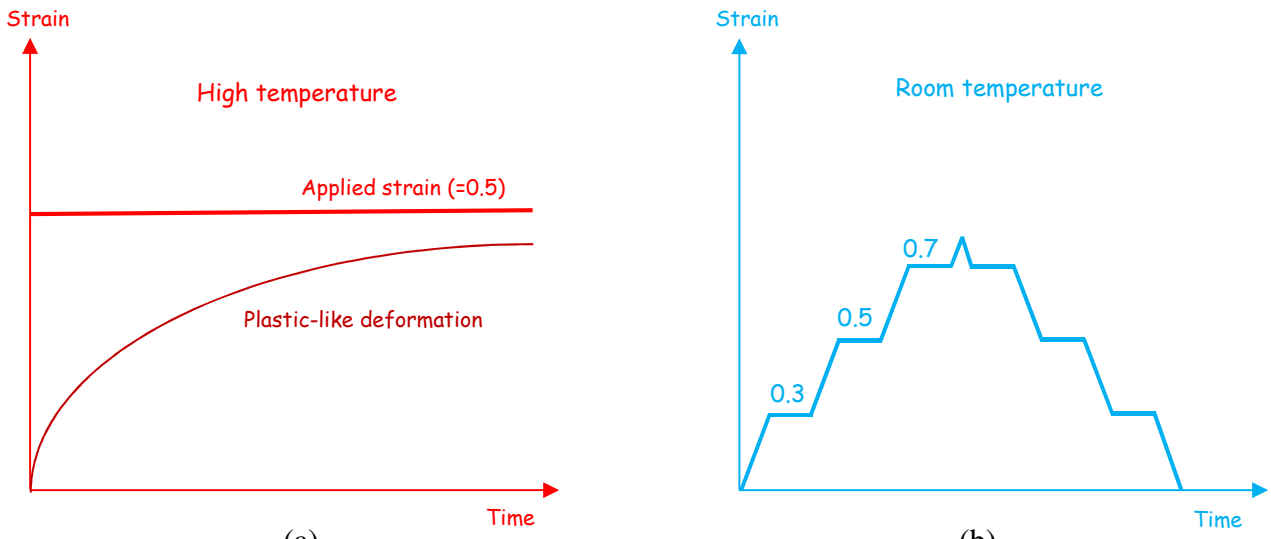

(a) (b)

Figure 4. Two-step loading condition: (a) relaxation at high temperature resulting in chemical relaxation followed by (b) (multi-step) relaxation at room temperature (in a loading-unloading cycle) resulting in physical relaxation.

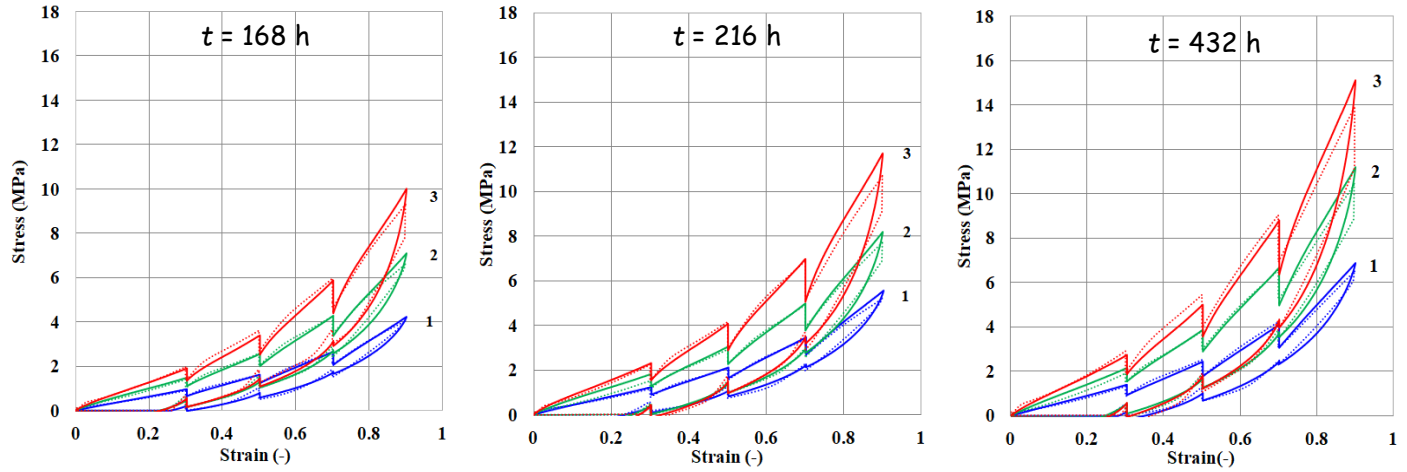

(a)

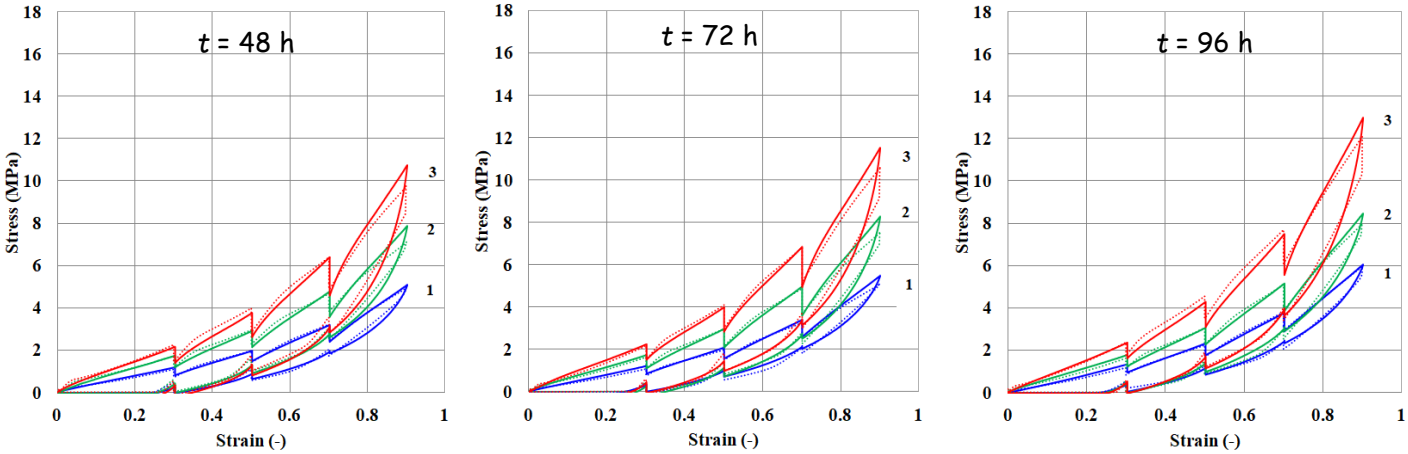

(b)

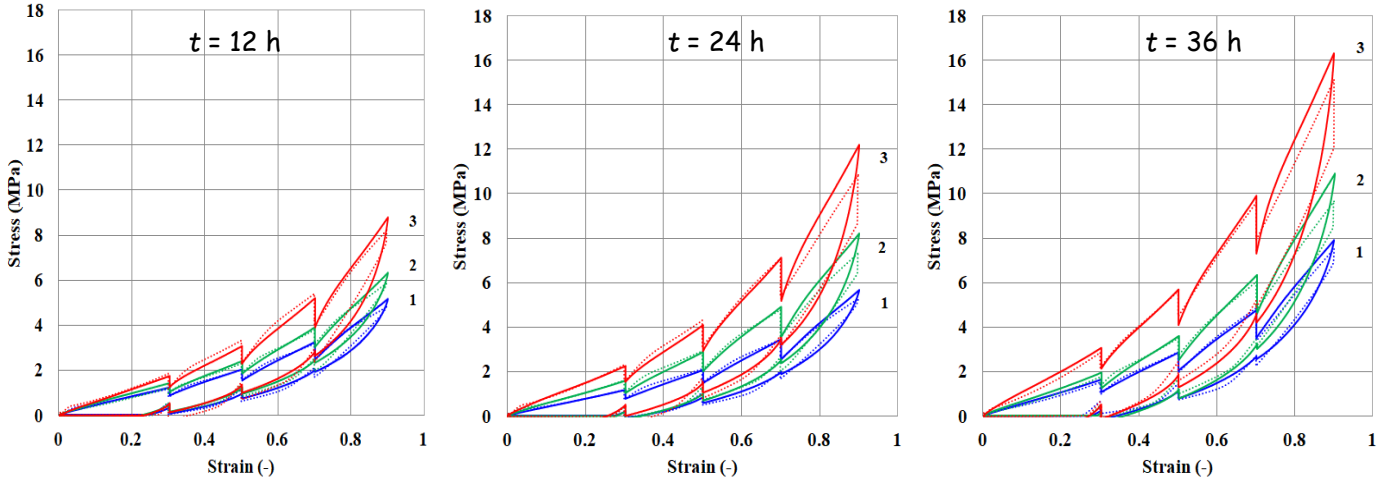

(c)

Figure 5. Multi-step stress relaxation responses at RT (solid lines: experiments, dashed lines: model) of thermally aged SBR (1: SBR15, 2: SBR25, 3: SBR43) under different exposure times t and aging temperatures: (a) $T = 383°K$, (b) $T = 403°K$, (c) $T = 423°K$. We refer the reader to Fig. 1 for the response of the unaged SBR.

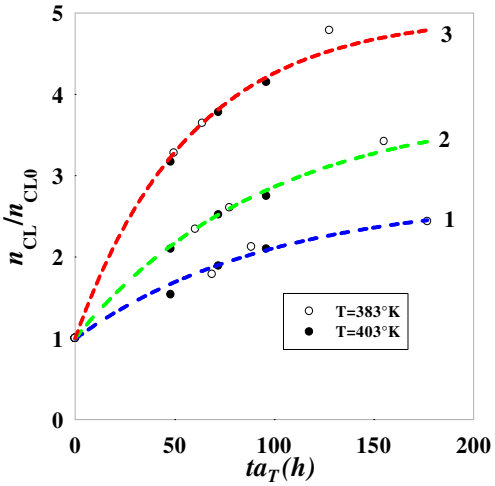

Figure 6. Alteration kinetics for the CL chains parameters (symbols: identified values, solid lines: Eq. (13)) of thermally aged SBR (1: SBR15, 2: SBR25, 3: SBR43).

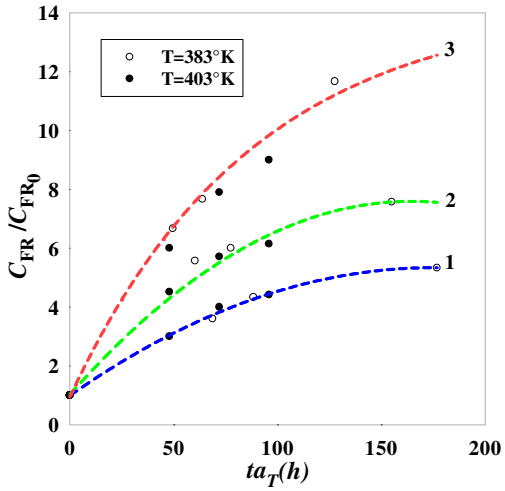

Figure 7. Alteration kinetics for the FR chains parameter C_{FR}/C_{FR0} (symbols: identified values, solid lines: Eq. (26)) of thermally aged SBR (1: SBR15, 2: SBR25, 3: SBR43).

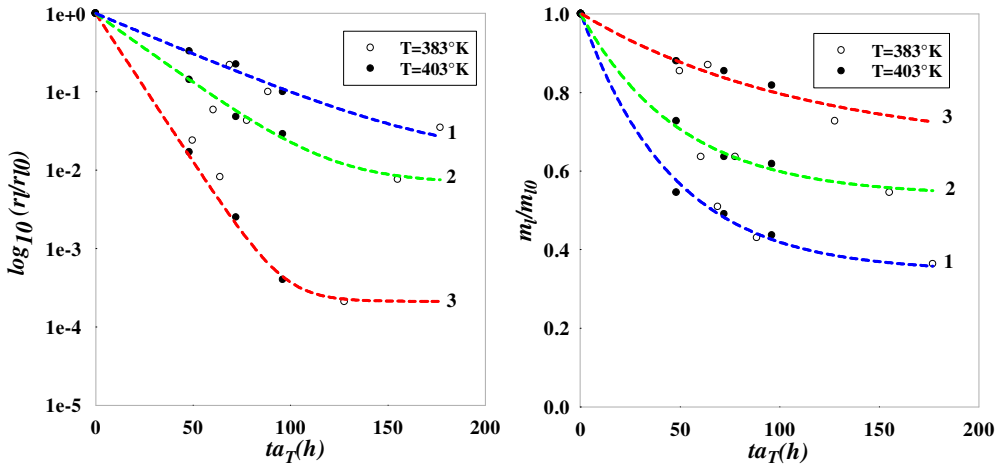

Figure 8. Alteration kinetics for the FR chains parameters r_l/r_{l0} and m_l/m_{l0} (symbols: identified values, solid lines: Eq. (26)) of thermally aged SBR (1: SBR15, 2: SBR25, 3: SBR43).

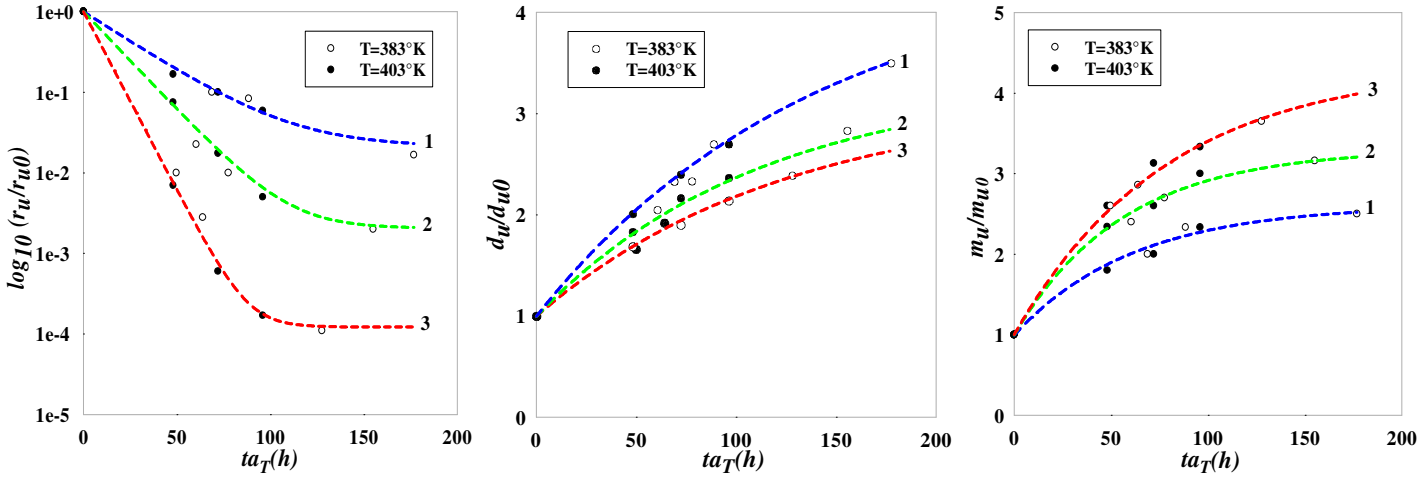

Figure 9. Alteration kinetics for the FR chains parameters r_u/r_{u0}, d_u/d_{u0} and m_u/m_{u0} (symbols: identified values, solid lines: Eq. (26)) of thermally aged SBR (1: SBR15, 2: SBR25, 3: SBR43).

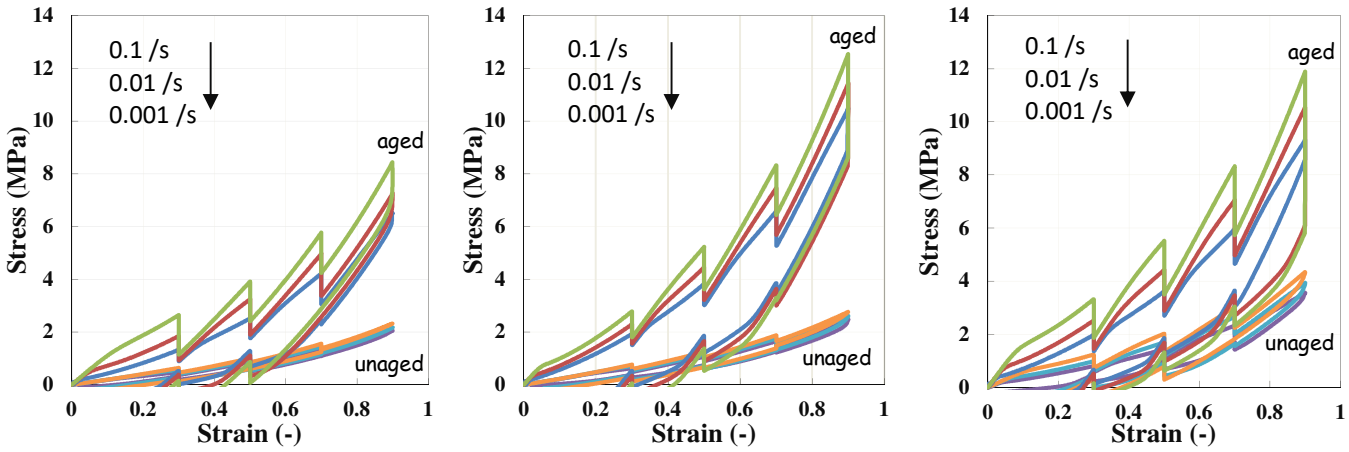

(a) (b) (c)

Figure 10. Model result of the aging effect on the rate-dependence of the response at RT: (a) SBR15 (aged at 483°K during 432h), (b) SBR25 (aged at 483°K during 432h), (c) SBR43 (aged at 483°K during 168h).

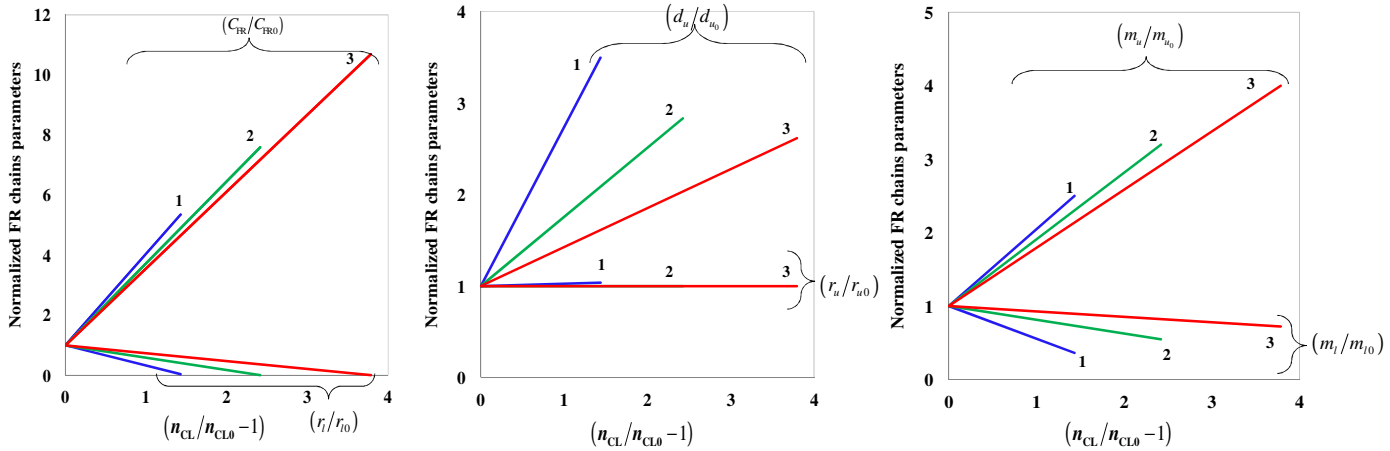

Figure 11. FR chains parameters vs. CL chains parameters (symbols: identified values, solid lines: Eq. (26)) of thermally aged SBR (1: SBR15, 2: SBR25, 3: SBR43).

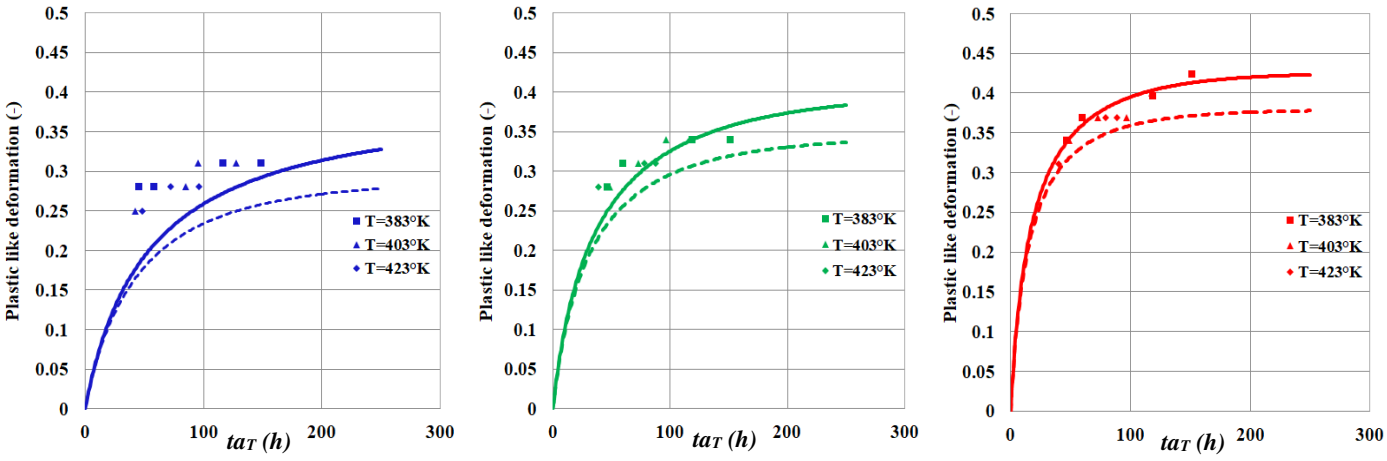

(a) (b) (c)

Figure 12. Model prediction of the plastic-like deformation: (a) SBR15, (b) SBR25, (c) SBR43 (symbols: experiments, solid lines: model prediction, dashed lines: model prediction including solely the newly born network).

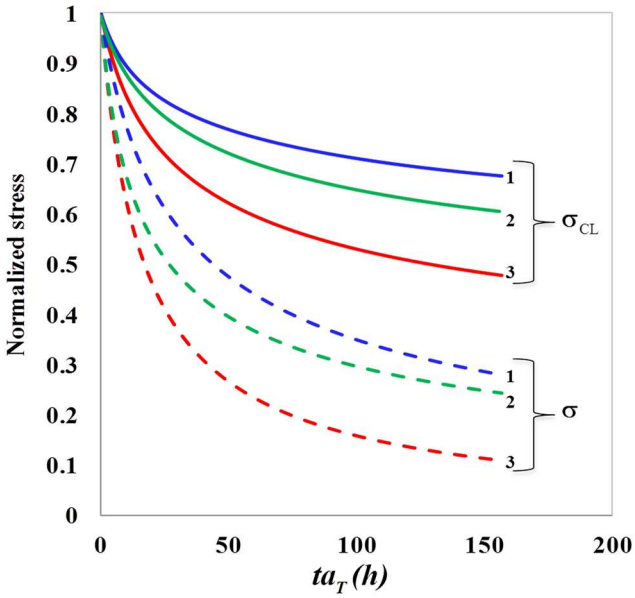

Figure 13. Model prediction of the chemical relaxation, σ_{CL} includes solely scission mechanism and σ combines scission and viscoelastic mechanisms (1: SBR15, 2: SBR25, 3: SBR43).